A comprehensive investigation of the strengthening effects of dislocations, texture and low and high angle grain boundaries in ultrafine grained AA6063 aluminum alloy

Najafi, S.; Eivani, A. R.; Samaee, M.; Jafarian, H. R.; Zhou, J.

DOI
10.1016/j.matchar.2017.12.004

Publication date
2018

Document Version
Accepted author manuscript

Published in
Materials Characterization

https://doi.org/10.1016/j.matchar.2017.12.004

A comprehensive investigation of the strengthening effects of dislocations, texture and low and high angle boundaries in ultrafine grained AA6063 aluminum alloy

S. Najafi [1], A.R. Eivani [1 *], M. Samaee [1], H.R. Jafarian [1], J. Zhou [2]

[1] School of Metallurgy and Materials Engineering, Iran University of Science and Technology (IUST), Tehran, Iran.

[2] Department of Biomechanical Engineering, Delft University of Technology, Mekelweg 2, 2628 CD Delft, The Netherlands

Abstract

The effect of equal channel angular pressing (ECAP) on the microstructure and mechanical properties of AA6063 aluminum alloy is investigated. For this purpose, samples of AA6063 aluminum alloy are deformed up to 10 passes using ECAP and the evolution of microstructure, texture and dislocation density is investigated. It is found that the dislocation density increases and cells mostly surrounded by low angle boundaries (LABs) form after 2 passes ECAP. Increasing the dislocation density continues with further processing and reaches a maximum at the 4th ECAP pass. With further deformation to 6 passes, the dislocation density reduces and the fraction of high angle boundaries (HABs) increases and the averages of cell size and grain size reduce, significantly, which indicates the occurrence

* Corresponding author; Email: aeivani@iust.ac.ir , Tel: +98 (0) 21 77 240 540, Fax: +98 (0) 21 77 240 480.

of grain refinement. However, a slight increase in dislocation density, average cell size (ACS) and average grain size (AGS) occur when 10 passes of ECAP are imposed. Hardness, yield (YS) and ultimate tensile strength (UTS) increase continuously although the most significant enhancement occurs after 2 passes ECAP. Investigating the correlation between the microstructure and mechanical properties indicate that Hall-Petch relationship is valid for UFG AA6063 before the coarsening starts and provided that the property is correlated to average cell size not the average grain size.

Keywords: Microstructure; Mechanical properties; Ultrafine grain; AA6063.

1 Introduction

Equal channel angular pressing (ECAP) [1–8] has shown tremendous capacity for producing ultrafine grained (UFG) materials. A long list of different materials, e.g., alloys of Al [2], Mg [9–11], Cu [12,13], Ti [14–16] and etc., which have been processed by ECAP for acquiring UFGs with ultrahigh strength can be presented. It can be said that many factors, e.g., chemical composition [17], crystal structure [14,18] and initial grain size [19,20], play role on the developed UFG structure and the obtained properties in different materials which are processed by ECAP.

Considering the fact that the chemical composition and grain structure of an industrially produced alloy, e.g., AA6063, can significantly vary [21] depending on the producer, different UFG structures and properties may be achieved. Therefore, it can be said that the development of microstructure and mechanical properties during severe plastic deformation depend on the traces of alloying elements. In addition, the initial conditions of the alloy, e.g., grain size, could have significant effects.

In general, nanostructured materials are produced to have elements in the size range of less than 100 nm and to indicate unique properties affected by the size. Similar story is valid for UFG materials. In fact, different and unusual properties have been reported to be acquired in UFG materials. One of these properties which has been reported to be changed during the production step of UFG materials is the correlation between microstructure and mechanical properties. In fact, while Hall-Petch relationship is valid for many engineering materials with conventional grain sizes [22], it has been frequently reported that this relationship destroys when the grain size reaches less than 1 μm, i.e., for nanocrystalline materials [23–26] and UFG materials [24,27,28].

In this investigation, the effect of ECAP on the development of UFG structure in AA6063 is investigated. It should be noted that the number of ECAP passes applied to this alloy has been limited to 6 elsewhere [20,29], which is due to the low workability of the alloy and occurrence of saturation after an equivalent strain of 3 to 4 [30]. However, it has been shown that with a small modification in die design, i.e., using a choke exit channel with an angle of 0.2 degrees, larger amounts of deformation is possible [31]. Owed to the modified design which has been used in this investigation, the deformation was continued up to 10 passes and the development of microstructure and mechanical properties was investigated. In addition to investigating the effect of UFG structure formation on mechanical properties, the correlation between microstructure and mechanical properties is investigated. Eventually, Hall-Petch relationship between the average grain size and the mechanical property of interest (hardness, yield strength and ultimate tensile strength) is validated.

2 Experimental procedure

AA6063 aluminum alloy with the chemical composition shown in Table 1 was received in the form of hot extruded rods of 80 mm diameter. 100 mm long cylindrical samples with a diameter of 20 mm were machined from the rods and annealed in an air circulating furnace at 550 °C for 30 min. Followed by annealing, the samples were water quenched. It was found that the initial annealing treatment is not efficient for producing circular recrystallized grain structure. Indeed, a recrystallized but slightly elongated grain structure forms after the initial annealing treatment at 550 °C for 30 min. Therefore, in order to produce an equiaxed grain structure, ECAP was initially performed for 2 passes and the samples were annealed at 550 °C for 6 hr. The samples were quenched in water after annealing treatment. ECAP was performed up to 10 passes with no rotation using a split die composed of two channels equal in cross section, intersecting at a 90 degrees angle with an outer curved corner of 22.5 degrees. With this die set-up, an equivalent strain of 1 is expected in each pass of ECAP [32,33]. Deformation was performed using a ram speed of 1 mm/sec. Then, ECAP was performed up to 10 passes with no rotation using a ram speed of 1 mm/sec.

Optical microscopy was used for revealing the microstructure of the sample after annealing. For this purpose, the sample was grinded after cutting, mechanically polished and anodized with HBF_4 solution at 20 V. The microstructure was observed with a polarized light microscope. X-ray diffraction was performed using Philips TW1730 machine at voltage of 40 kV with Cu K_α radiation, applying a 0.05 degrees step size.

Table 1: Chemical composition of the AA6063 alloy used in this study.

Element (wt. %)	Al	Mg	Si	Fe	Cu	Mn	Cr	Zn	Ti

AA6063 used in this study	Balance	0.84	0.57	0.31	0.03	0.04	0.03	0.10	0.03
Nominal composition of AA6063	Balance	0.45-0.9	0.2-0.6	Max 0.35	Max 0.1	Max 0.1	Max 0.1	Max 0.1	Max 0.1

Brinell hardness was measured on a plane normal to the ECAP direction. 20 indentations were made for each sample and the average value was obtained. Tensile testing was performed on sub-sized flat specimens according to ASTM E8. All the dimensions were reduced by 50% due to size limit. The total length of the tensile specimen was 50 mm and the gauge length was 12.5 mm. The width of the sample was 3 mm and the thickness was 2 mm. A SANTAM universal testing machine was used at a crosshead speed of 0.7 mm/min.

In order to observe the microstructure of the samples after ECAP and to reveal subgrain boundaries, JEOL 7100F scanning electron microscope (SEM) equipped with electron backscattered diffraction (EBSD) set-up was used (accelerating voltage: 15 kV; tilt angle: 70 °; working distance: 15 mm; step sizes: 0.05 μm). For this purpose, samples were initially grinded and then electropolished at 20 V; 10 sec; flow rate: 15; electrolyte: 700ml CH_3OH + 300 ml HNO_3; temperature: 243 K. Orientation contrast data were analyzed with the TSL OIM analysis software.

3 Results and discussion

3.1 Microstructure evolution

3.1.1 Substructure formation

The initial microstructure after annealing at 550 °C for 6 hr is a coarse structure with an average grain size larger than 1000 µm [29]. The effect of 2, 6 and 10 passes ECAP on the evolution of microstructure is shown in Fig. 1. Low angle boundaries (LABs) and high angle boundaries (HABs) are indicated by red and black lines, respectively. It is found that a typical cell structure has formed after 2 passes ECAP. The cells are mostly surrounded by LABs. The average cell size (ACS) and average grain size (AGS) are 1.12 and 3.24 µm, respectively. For this measurement, those cells which are totally surrounded by HABs are considered as grains and the rest as cells. Results of Image analyzer shown in Table 2 indicate that the fraction of HABs and LABs are 34 and 66 %, respectively. These characteristics indicate that although cell structure around the size range of 1 µm has formed, but it cannot be said that an ultrafine grained (UFG) material has been produced.

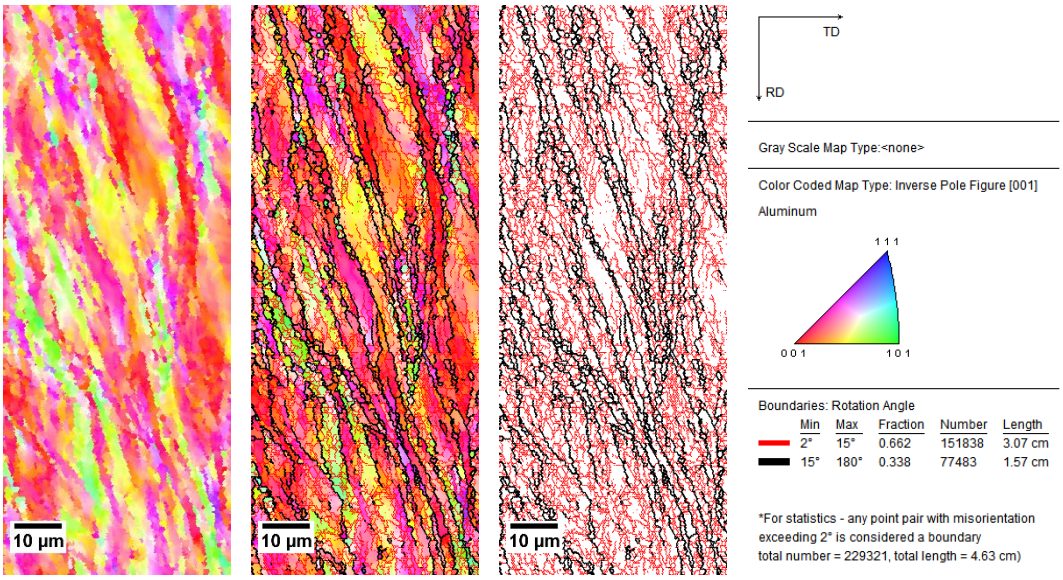

(a)

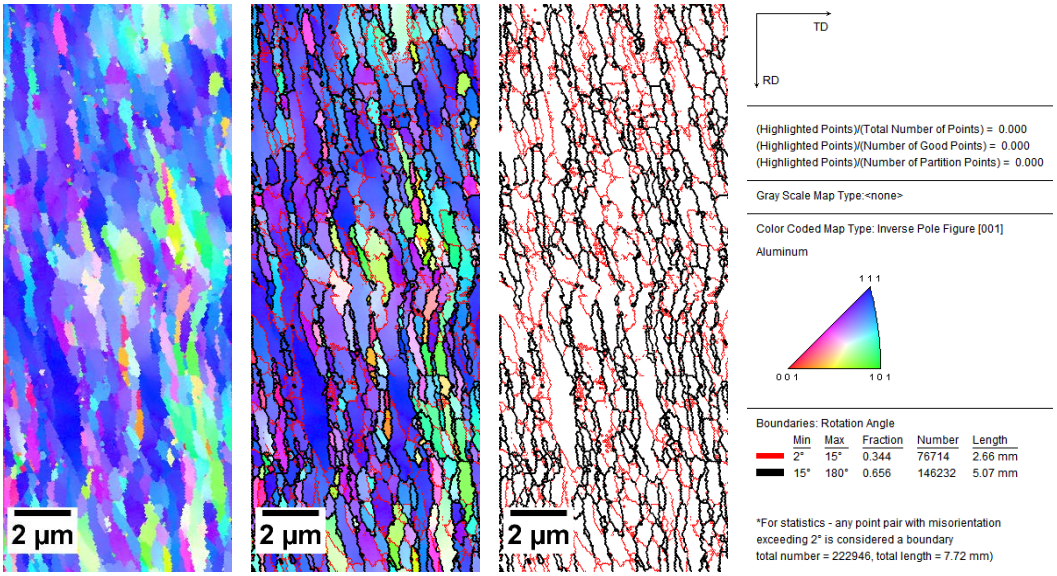

(b)

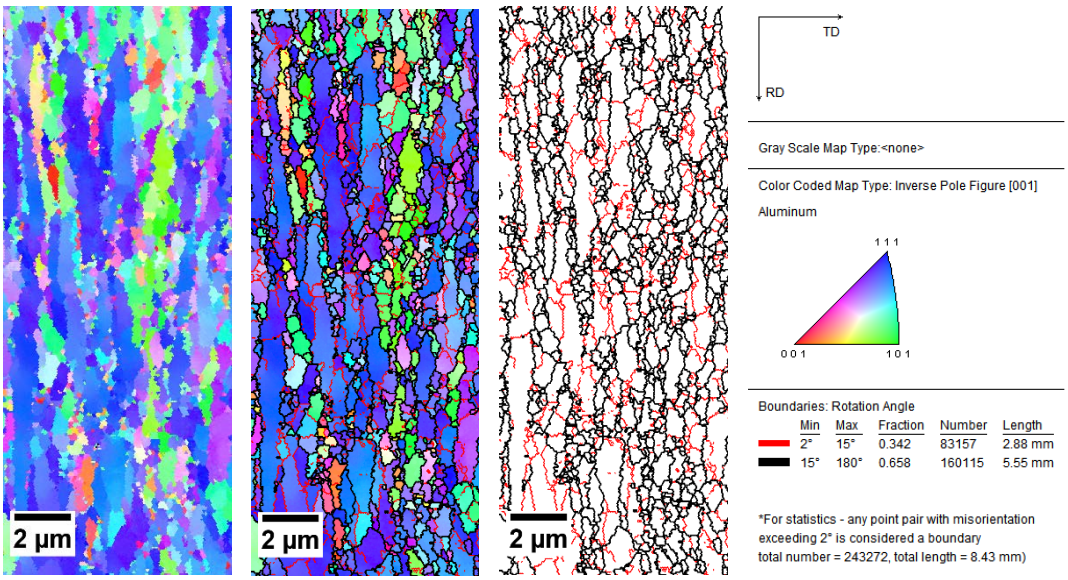

(c)

Figure 1- EBSD color maps of the microstructures after (a) 2, (b) 6 and (c) 10 passes ECAP.

In order to see how the situation changes with further deformation, Fig. 1 (b) should be considered. It can be seen that the cells are further refined with regard to those in 2 pass deformed sample and the ACS reaches to 425 nm. In addition, the fraction of HABs increases to 66 %, which shows almost 100 % increase. This shows that the structure is moving towards formation of a recrystallized UFG structure. However, it is found that further increase in the number of passes is not effective on the development of nanostructure. In fact,

the ACS is 662 nm after 10 passes ECAP. This shows that the ACS has slightly increased when further deformation is applied. In other words, coarsening of cell and grain structure occurs in this sample. Similar behavior has been observed for AGS as presented in Table 2. At the same time, the fraction of HABS is almost unchanged at 66 %. Increasing the ACS in Al alloys with increasing deformation has been previously observed in pure Al [34–36]. This phenomenon has been previously attributed to high stacking fault energy (SFE) of aluminum alloys that encourage occurrence of dynamic recovery [34–36].

Table 2- Characteristics of the microstructures observed in Fig. 1.

Sample	AGS (μm)	ACS (nm)	Fraction of HABs (%)
2 pass	3.244	1119	34
6 pass	0.425	251	66
10 pass	0.662	329	66

3.1.2 Texture evolution

Fig. 2 shows the (1 0 0), (1 1 0) and (1 1 1) pole figures of samples after different number of ECAP passes. Two ECAP passes led to the formation of A ideal texture component and B fibre texture also oriented parallel to the shear direction (⟨110⟩||SD). According to (1 1 1) pole figure, a texture close to ideal shear texture can be seen after 2 passes; whereas after more passes, a deviation from ideal shear texture is observable. This deviation can be assumed to be attributed to the successive change of shear plane and the retained texture that accumulates with increasing number of ECAP passes [39]. ECAP processing also leads to the development of an inhomogeneous shear texture after initial passes; although up to 10 repetitive passes cause texture homogenization [40]. In addition, the (1 1 1) pole figure shows maximum sensitivity of 2.37 for 2 passes ECAPed samples. On the other hand, B fibers along

with weak A fibers exist in the texture. With increasing number of ECAP passes to 6, sensitivity increased to 3.17 with A fibers getting removed while B fibers were increasing. After 10 passes ECAP, the maximum sensitivity reached to 5.28, A fibers were completely removed and B fibers strongly existed in the texture. The same trend can be seen in (110) plane which means weak fibers exist in the texture at the beginning while with increasing number of passes, strong B fibers are formed.

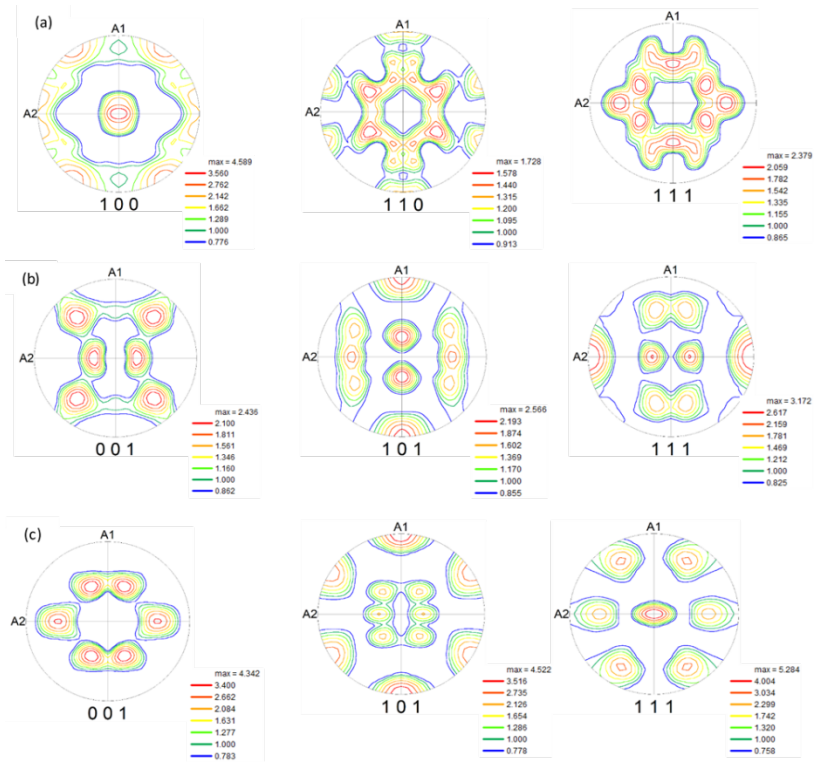

Figure 2- (100), (110) and (111) pole figures for samples ECAPed to 2, 6 and 10 passes in (a), (b) and (c), respectively.

Fig. 3 represents the orientation distribution function (ODF) plots with constant ϕ 2 sections. According to ODF results, the maximum sensitivity in 2nd pass is reported 5.43 and it increased to 6.93 with increasing ECAP pass numbers to 6. It reached to its maximum amount (13.97) after 10 passes. Besides, the more the sensitivity is, the stronger the texture becomes and it accounts for more homogenous texture distribution after the early passes. This

more sensitivity also represents more severe deformation and as a result, finer grains which lead to inherit the same deformation texture.

Based on these results, texture variations significantly depend on how many times the sample is pressed through the ECAP die. Furthermore, the axial compression deformation affects the texture quite dramatically and this change is stronger for the samples with higher number of ECAP passes. In addition, due to the applied strain and shear band formation, grains rotated against the matrix which resulted in fine grained microstructure. This means that because of working temperature, recrystallization is less probable and the predominant mechanism is grain subdivision which is a result of high applied shear strain caused by ECAP processing.

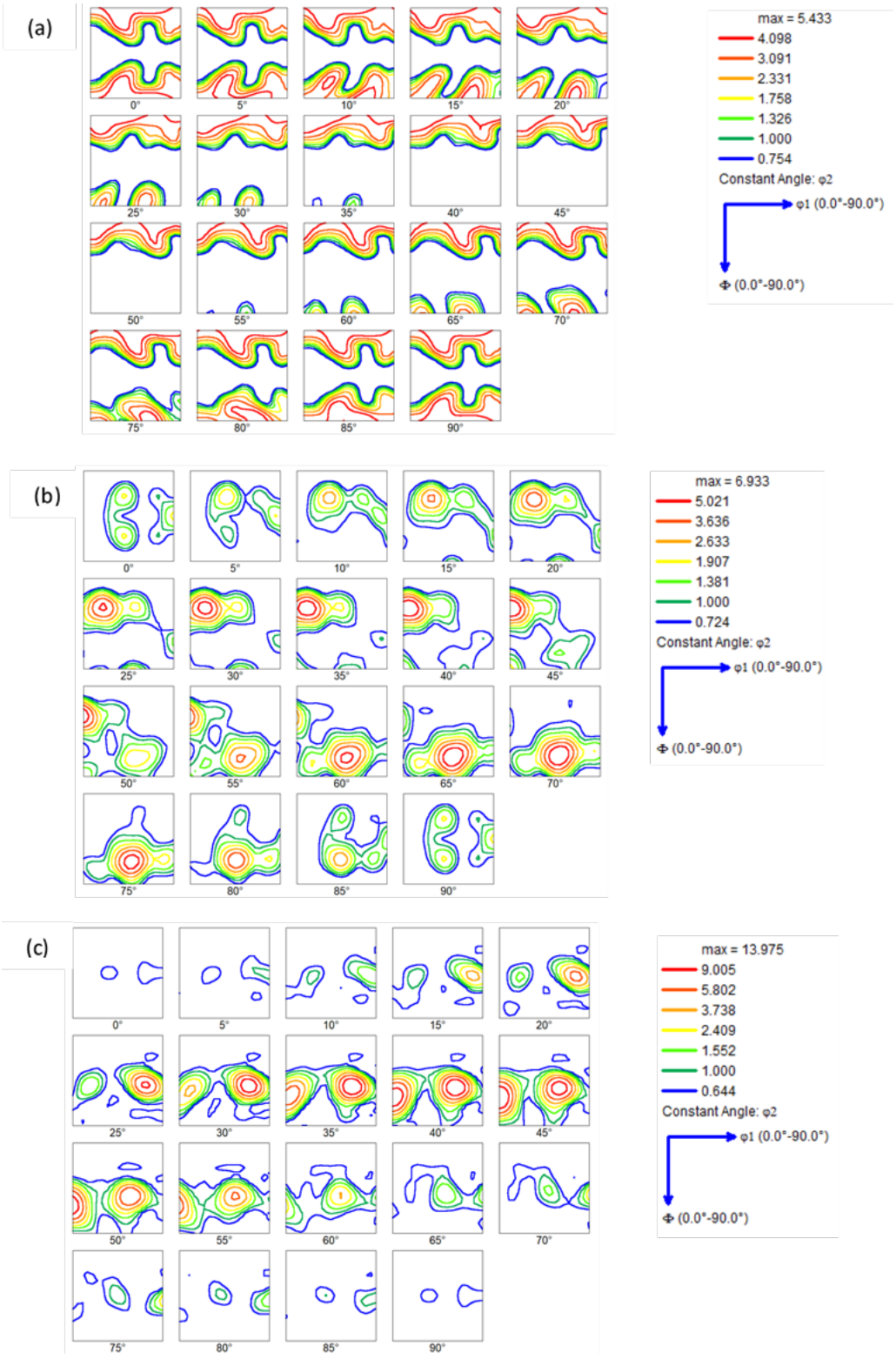

Figure 3- Orientation distribution function (ODF) plots for constant ϕ2 for samples ECAPed to 2, 6 and 10 passes in (a), (b) and (c) respectively.

3.1.3 Dislocation density

XRD analysis was performed in order to calculate the dislocation density and its evolution during ECAP processing. The results of XRD analysis is shown in Fig. 4. All of the XRD patterns are similar which shows no change in phase constitution, which are all composed of a single aluminum phase. However, the intensities of the peaks are changed and peak broadening is observed which results in variations in dislocation denisty.

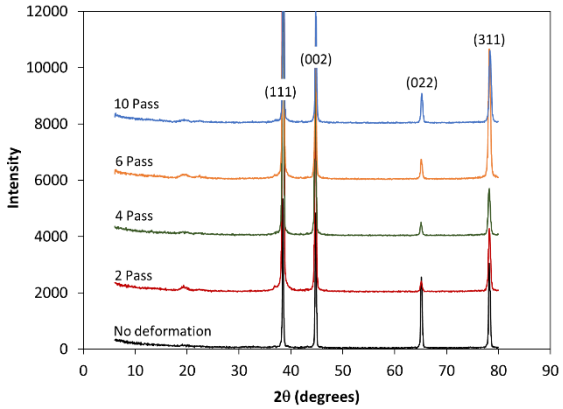

Figure 4- Results of XRD analysis on the samples prior to and after ECAP deformation.

Variations in dislocation density in the alloy is shown in Fig. 5. The dislocation density in the un-deformed samples has been considered to be similar, i.e., $1*10^{6}$ cm^{-2}, whether the samples are air cooled or water quenched. However, with applying two passes deformation, the dislocation density in WQ sample goes higher than the AC sample. This may be attributed to the fact that the concentration of alloying elements, e.g., Mg and Si, is higher in the WQ samples. It is well-known that the higher concentration of Mg results in further dislocation multiplication and work-hardening in addition to grain refinement. The dislocation density continues to increase in AC sample which is in line with increasing the amount of deformation leading further dislocation multiplication. However, a reduction in dislocation density of the WQ samples is observed in the 6 pass ECAP alloy which continues to a more significant reduction when the number of passes is increased to 10.

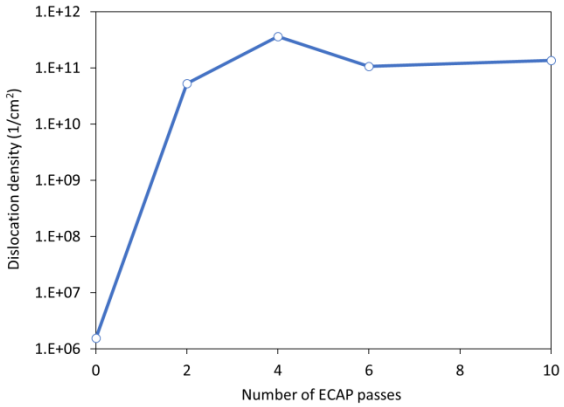

Figure 5- Variations in dislocation density as a result of ECAP deformation prior to aging in AC and WQ samples.

This reduction in dislocation density in the samples with 4 and 6 passes ECAP, is in line with formation of an ultrafine grained structure which is observed in the sample with 6 passes deformation. Indeed, the formation of an ultrafine grain structure with a relatively high fraction of HAGBs, has resulted in reduction in dislocation density. In other words, the dislocations are supposed to be consumed for this purpose. After 10 passes ECAP, the ACS and AGS slightly increase while the fraction of HAGBs remains unchanged and a slight increase in dislocation density is observed. These are two different phenomena which are occurring with increasing the number of passes. In fact, the increase in the AGS and ACS may be attributed to occurrence of dynamic recovery, based on which, a reduction in dislocation density may be expected. However, since the deformation is continued, the dislocation density may increase as well. The net result of reducing the dislocation density due to dynamic recovery and increasing due to proceeding deformation, is a slight increase in dislocation density and a successive increase in strength. Therefore, a continuous increase in mechanical properties is likely to occur.

3.2 Mechanical properties

3.2.1 Hardness

Hardness of the sample in as-annealed condition and after 2, 4, 6 and 10 passes ECAP has been shown in Fig. 6. Hardness shows an initial sharp increase with the first two passes of deformation and then continues with gradual increase. Saturation of the microstructure has been previously observed for this alloy after an equivalent strain around 3-4 [30]. In addition, it is claimed that when this alloy is deformed up to 6 passes ECAP, hardness reaches an unchanged value [20,37]. However, no sign of saturation of the hardness is observed in this case although the alloy system is similar to that used in [20,37]. This is against the existing literature [20,30,37] and may be attributed to activation of re-strengthening mechanism [41] and the role of higher Mg content in solid solution [17] in comparison to the alloy and treatment used in [20,37]. Activation of re-strengthening mechanisms [41] by increasing number of passes may be an effective parameter, especially in the sample which has been deformed for 10 passes. Indeed, it has been previously observed that significant increase in the number of ECAP deformation passes may result in further and more significant grain refinement with changing the refinement mechanism. In fact, in [20], the samples have been cooled in the air after annealing at 550 °C for 6 hr and therefore, lower amount of Mg would be in solid solution. Higher concentration of Mg in solid solution can as well interpret the lower values obtained for ACSs [17] and higher hardness.

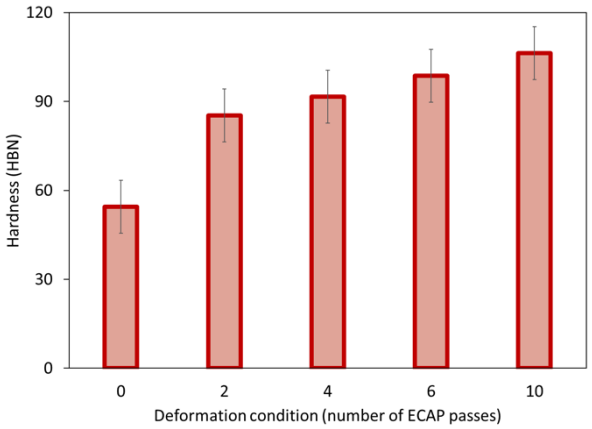

Figure 6- Variation in hardness of the samples as a result of deformation.

3.2.2 Tensile properties

Engineering stress strain curves of the alloy in as-annealed condition and after 2, 4, 6 and 10 passes ECAP are shown in Fig. 7. The material shows the highest elongation to failure (e_f) and uniform elongation (e_u) in as-annealed condition. It is clear that elongation reduces with deformation while the flow stress is found to increase with deformation. Extracted values for 0.2 % yield strength (YS) and ultimate tensile strength (UTS) are shown in Fig. 8. YS shows 200 % increase with the first two passes of deformation while there is about 61 % increase for UTS. This indicates a significant increase in YS and a considerable increase in UTS with two passes ECAP. However, both YS and UTS increase moderately with further deformation. This is 30 and 26 % enhancements in YS and 24 and 27 % enhancements in UTS with 6 and 10 passes ECAP.

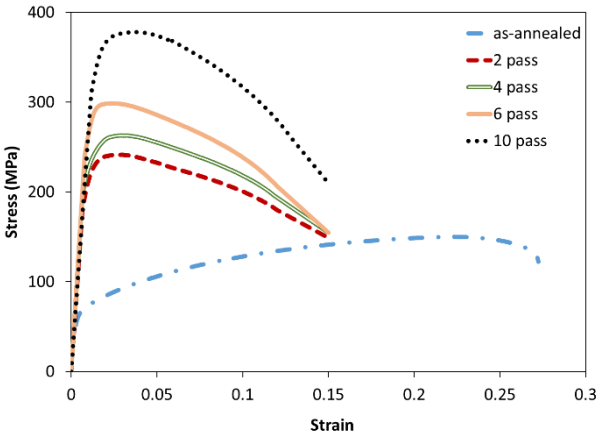

Figure 7- Engineering stress-strain tensile test results in as-annealed condition and after 2, 4, 6 and 10 passes ECAP.

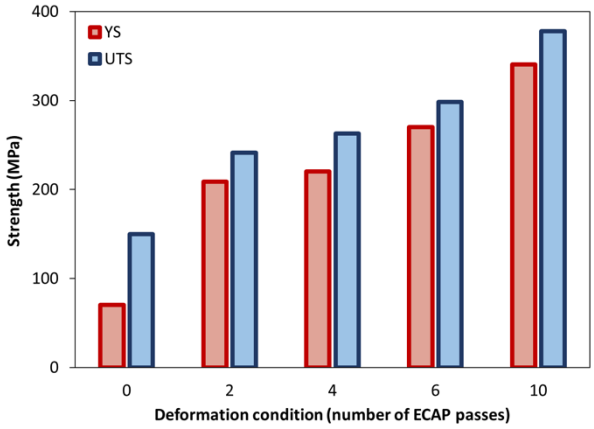

Figure 8- Extracted YS and UTS from tensile test graphs in Fig. 7.

3.3 Correlation between microstructure and tensile properties

Hall-Petch relationship is used in order to investigate the correlation between microstructure and mechanical properties. Hall-Petch relationship which is shown in Eq. (1) is a general relationship between hardness, YS or UTS and the grain size of a metallic material [22].

$$\sigma_0 = \sigma_i + \frac{k}{\sqrt{D}} \qquad \text{Eq. (1)}$$

where σ_0 is the property of interest, i.e., hardness, YS or UTS, σ_i the friction stress, k locking parameter and D grain diameter. It has been reported in the literature [23–28] that this relationship destroys when the size of the microstructure comes in the range of UFG

materials, i.e., less than 1 µm. The aim of this part of the research is to investigate whether the relationship is valid for the UFG AA6063 alloy or not. For this purpose, the graph of σ_0 vs. $D^{-1/2}$ is drawn in Fig. 9. Two values, i.e., average grain size (AGS) and average cell size (ACS), have been used instead of D. In addition, the graphs are presented two times. Once with the property data up to 10 passes and once with the data up to 6 passes ECAP. It can be seen in Figs. 9 (a) and (b) that there is no linear relationship between σ_0 and $AGS^{-1/2}$ to indicate the validity of Hall-Petch relationship. This observation is indeed valid for samples after 6 or 10 passes of ECAP. Similar results are found in Fig. 9 (c) for the correlation between σ_0 and $ACS^{-1/2}$ when the property of the material up to 10 passes ECAP is considered. However, when the data related to the sample which has been processed for 10 passes is deleted, a linear relationship between the σ_0 and $ACS^{-1/2}$ is observed. This indicates that the Hall-Petch relationship is valid for determination of the correlation between microstructure and mechanical properties, before the saturation of the microstructure, i.e., up to 6 passes ECAP. In addition, what can represent D in Eq. (1), is the ACS in which the cells and LABs are as well counted for calculation.

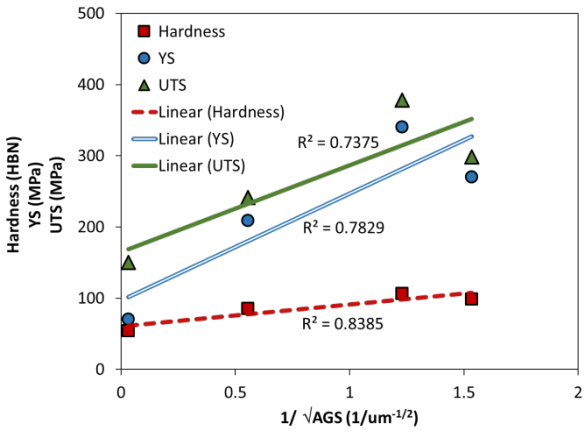

(a)

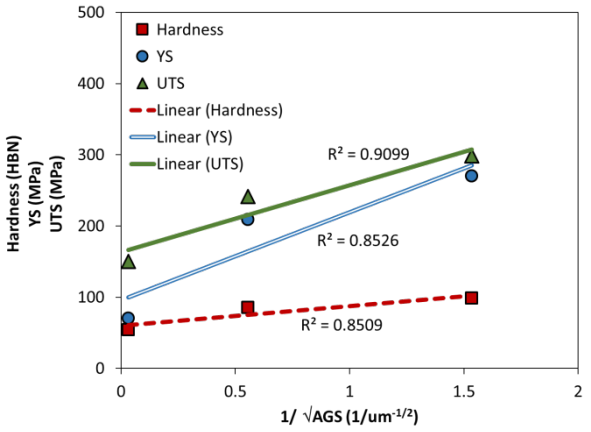

(b)

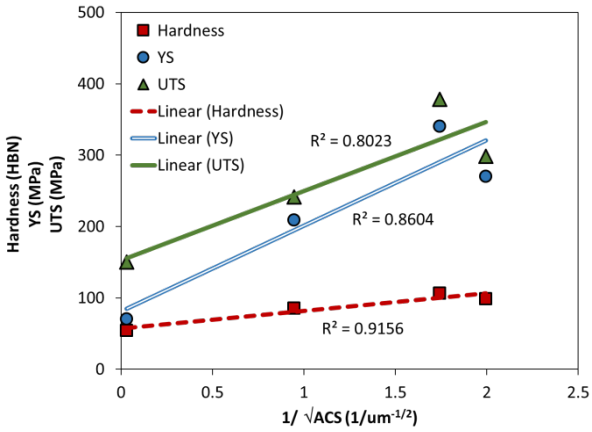

(c)

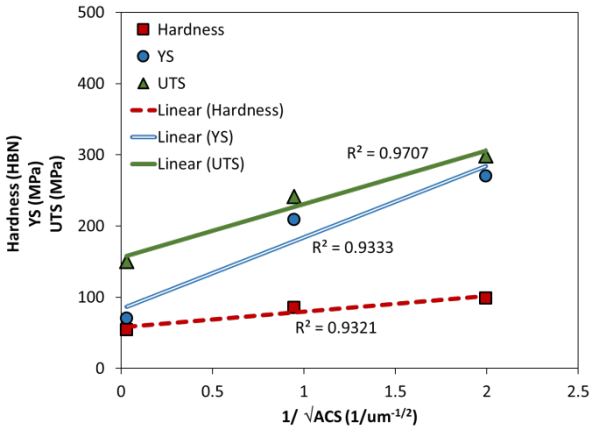

(d)

Figure 9- Validation of Hall-Petch relationship for hardness, yield strength and ultimate tensile strength with (a) average grain size up to 10 passes deformation, (b) average grain size up to 6 passes deformation, (c) average cell size up to 10 passes deformation, (d) average cell size up to 6 passes deformation.

If the Hall-Petch equation is valid for determination of the correlation between average grain size and the mechanical property of interest, the value of the coefficient of determination (R^2) for linear regression between σ_0 vs $D^{-1/2}$ should be as close to 1 as possible. These values for the graphs shown in Fig. 9 are presented in Table 3. It can be seen that the value of R^2 is normally smaller than 0.9 which shows a very small probability for existence of linear relationship between σ_0 vs $D^{-1/2}$ for Figs. 9 (a) to (c). However, an acceptable agreement exists between the results which have been shown in Fig. 9 (d) which represent the correlation between σ_0 vs $ACS^{-1/2}$ before the microstructure has been saturated. From statistical point view [38], the probability of completely uncorrelated σ_0 vs $ACS^{-1/2}$ is less than 1% for correlation coefficient in the range of R^2=0.938-0.932 for three data used for fitting. It shows that the correlation between the two quantities is very significant.

Table 3- Values of coefficient of determination (R2) extracted from Fig. 9.

Validation	Hardness	YS	UTS
AGS – 10 pass	0.8385	0.7829	0.7375
AGS – 6 pass	0.8509	0.8520	0.9099
ACS – 10 pass	0.9156	0.8604	0.8023
ACS – 6 pass	0.9321	0.9333	0.9707

An important phenomenon which may be studied from the graphs shown in Fig. 9 is variations in the locking parameter, k in Eq. (1). This parameter is a factor which can be used to measure the relative hardening contribution of the grain boundaries and can be extracted from the slope of the plots in Fig. 9. It can be seen that when the data of the sample with 10 passes of deformation are added into the fitting process, a larger slope is observed, i.e., a

larger k parameter. This indeed indicates that a more significant grain boundary hardening has occurred when larger number of deformation passes are applied. Another important parameter which is found to have effect on the slope of the graphs is whether the fitting is performed with AGS or ACS. Indeed, as the k parameter is related to the effectiveness of the boundaries to inhibit dislocation motions, the subgrain boundaries are as well expected to be effective in strengthening and led to variations in the slope. Therefore, this may be used as a good explanation for the fact that the observations provided in this investigation indicate reliable application of Hall-Petch relationship when the cells and subgrains are as well considered.

4 Conclusions

In this investigation, the effect of up to 10 passes of ECAP on the evolution of microstructure, textures, dislocation density, hardness and tensile properties of AA6063 alloy is investigated.

1- It is found that ultrafine grained (UFG) structure forms in AA6063 aluminum alloy with 6 passes of deformation. With further deformation, the average cell size slightly increases.
2- It is observed that with increasing the number of passes, the dislocation density increases up to 4 passes and reduces afterwards.
3- The occurrence of the reduction in dislocation density is in line with formation of an ultrafine grain structure with high angle boundaries.
4- Despite of increasing average cell and grain size with deformation up to 10 passes, mechanical properties, i.e., hardness and tensile properties, are found to continue to increase up to 10 passes deformation.

5- Hall-Petch relationship is valid for UFG AA6063 before the coarsening of the microstructure occurs after 10 passes ECAP and provided that the property is correlated to average cell size not the average grain size.

5 Acknowledgment

The authors would like to thank Prof. Nobuhiro Tsuji, Kyoto University, Japan, for providing equipment for EBSD analysis. The authors also thankful from Japan Student Services Organization (JASSO) for their support by Follow-up Research Fellowship in fiscal year of 2015.

6 References

[1] M. Furukawa, Z. Horita, M. Nemoto, T.G. Langdon, Review: processing of metals by equal-channel angular pressing, J. Mater. Sci. 36 (2001) 2835–2843.

[2] Z. Horita, T. Fujinami, M. Nemoto, T.G. Langdon, Equal-channel angular pressing of commercial aluminum alloys: grain refinement, thermal stability and tensile properties, Metall. Mater. Trans. A. 31 (2000) 691–701.

[3] Y. Iwahashi, Z. Horita, M. Nemoto, T.G. Langdon, An investigation of microstructural evolution during equal-channel angular pressing, Acta Mater. 45 (1997) 4733–4741.

[4] Y. Iwahashi, Z. Horita, M. Nemoto, T.G. Langdon, The process of grain refinement in equal-channel angular pressing, Acta Mater. 46 (1998) 3317–3331.

[5] Y. Iwahashi, J. Wang, Z. Horita, M. Nemoto, T.G. Langdon, Principle of equal-channel angular pressing for the processing of ultra-fine grained materials, Scr. Mater. 35 (1996) 143–146.

[6] T.G. Langdon, M. Furukawa, M. Nemoto, Z. Horita, Using equal-channel angular pressing for refining grain size, Jom. 52 (2000) 30–33.

[7] K. Nakashima, Z. Horita, M. Nemoto, T.G. Langdon, Influence of channel angle on the development of ultrafine grains in equal-channel angular pressing, Acta Mater. 46 (1998) 1589–1599.

[8] R.Z. Valiev, T.G. Langdon, Principles of equal-channel angular pressing as a processing tool for grain refinement, Prog. Mater. Sci. 51 (2006) 881–981.

[9] K. Xia, J.T. Wang, X. Wu, G. Chen, M. Gurvan, Equal channel angular pressing of magnesium alloy AZ31, Mater. Sci. Eng. A. 410 (2005) 324–327.

[10] W.J. Kim, C.W. An, Y.S. Kim, S.I. Hong, Mechanical properties and microstructures of an AZ61 Mg Alloy produced by equal channel angular pressing, Scr. Mater. 47 (2002) 39–44.

[11] K. Máthis, J. Gubicza, N.H. Nam, Microstructure and mechanical behavior of AZ91 Mg alloy processed by equal channel angular pressing, J. Alloys Compd. 394 (2005) 194–199.

[12] S. Qu, X.H. An, H.J. Yang, C.X. Huang, G. Yang, Q.S. Zang, Z.G. Wang, S.D. Wu, Z.F. Zhang, Microstructural evolution and mechanical properties of Cu–Al alloys subjected to equal channel angular pressing, Acta Mater. 57 (2009) 1586–1601.

[13] A. Vinogradov, V. Patlan, Y. Suzuki, K. Kitagawa, V.I. Kopylov, Structure and properties of ultra-fine grain Cu–Cr–Zr alloy produced by equal-channel angular pressing, Acta Mater. 50 (2002) 1639–1651.

[14] Y.G. Ko, W.S. Jung, D.H. Shin, C.S. Lee, Effects of temperature and initial microstructure on the equal channel angular pressing of Ti–6Al–4V alloy, Scr. Mater. 48 (2003) 197–202.

[15] D.H. Shin, I. Kim, J. Kim, Y.S. Kim, S.L. Semiatin, Microstructure development during equal-channel angular pressing of titanium, Acta Mater. 51 (2003) 983–996.

[16] I.P. Semenova, G.I. Raab, L.R. Saitova, R.Z. Valiev, The effect of equal-channel angular pressing on the structure and mechanical behavior of Ti–6Al–4V alloy, Mater. Sci. Eng. A. 387 (2004) 805–808.

[17] Y. Iwahashi, Z. Horita, M. Nemoto, T.G. Langdon, Factors influencing the equilibrium grain size in equal-channel angular pressing: Role of Mg additions to aluminum, Metall. Mater. Trans. A. 29 (1998) 2503–2510.

[18] S.L. Semiatin, D.P. DeLo, Equal channel angular extrusion of difficult-to-work alloys, Mater. Des. 21 (2000) 311–322.

[19] M. Samaee, S. Najafi, A.R. Eivani, H.R. Jafarian, J. Zhou, Simultaneous improvements of the strength and ductility of fine-grained AA6063 alloy with increasing number of ECAP passes, Mater. Sci. Eng. A. 669 (2016) 350–357.

[20] S. Valipour, A.R. Eivani, H.R. Jafarian, S.H. Seyedein, M.R. Aboutalebi, Effect of pre-deformation thermomechanical processing on the development of ultrafine grain structure during equal channel angular extrusion, Mater. Des. 89 (2016) 377–384.

[21] A.S.M. International, A.I.H. Committee, A.I.A.P.D. Committee, Metals Handbook: Properties and selection, Asm International, 1990.

[22] R.W. Armstrong, The influence of polycrystal grain size on several mechanical properties of materials, Metall. Mater. Trans. 1 (1970) 1169–1176.

[23] K.E. Aifantis, A.A. Konstantinidis, Hall–Petch revisited at the nanoscale, Mater. Sci. Eng. B. 163 (2009) 139–144. doi:10.1016/j.mseb.2009.05.010.

[24] P. Bazarnik, Y. Huang, M. Lewandowska, T.G. Langdon, Structural impact on the Hall–Petch relationship in an Al–5Mg alloy processed by high-pressure torsion, Mater. Sci. Eng. A. 626 (2015) 9–15. doi:10.1016/j.msea.2014.12.027.

[25] A.H. Chokshi, A. Rosen, J. Karch, H. Gleiter, On the validity of the Hall-Petch relationship in nanocrystalline materials, Scr. Metall. 23 (1989) 1679–1683.

[26] G.J. Fan, H. Choo, P.K. Liaw, E.J. Lavernia, A model for the inverse Hall–Petch relation of nanocrystalline materials, Mater. Sci. Eng. A. 409 (2005) 243–248. doi:10.1016/j.msea.2005.06.073.

[27] M. Furukawa, Z. Horita, M. Nemoto, R.Z. Valiev, T.G. Langdon, Microhardness measurements and the Hall-Petch relationship in an Al □Mg alloy wit grain size, Acta Mater. 44 (1996) 4619–4629.

[28] A. Loucif, R.B. Figueiredo, T. Baudin, F. Brisset, R. Chemam, T.G. Langdon, Ultrafine grains and the Hall–Petch relationship in an Al–Mg–Si alloy processed by high-pressure torsion, Mater. Sci. Eng. A. 532 (2012) 139–145. doi:10.1016/j.msea.2011.10.074.

[29] M.S. Shadabroo, A.R. Eivani, H.R. Jafarian, S.F. Razavi, J. Zhou, Optimization of interpass annealing for a minimum recrystallized grain size and further grain refinement towards nanostructured AA6063 during equal channel angular pressing, Mater. Charact. 112 (2016) 160–168. doi:10.1016/j.matchar.2015.12.018.

[30] M. Das, G. Das, M. Ghosh, M. Wegner, V. Rajnikant, S. GhoshChowdhury, T.K. Pal, Microstructures and mechanical properties of HPT processed 6063 Al alloy, Mater. Sci. Eng. A. 558 (2012) 525–532.

[31] M. Torabi, A.R. Eivani, H. Jafarian, M.T. Salehi, Die Design Modification to Improve Workability during Equal Channel Angular Pressing, Adv. Eng. Mater. 18 (2016) 1469–1477.

[32] A.R. Eivani, A.K. Taheri, The effect of dead metal zone formation on strain and extrusion force during equal channel angular extrusion, Comput. Mater. Sci. 42 (2008) 14–20.

[33] A.R. Eivani, A.K. Taheri, A new method for estimating strain in equal channel angular extrusion, J. Mater. Process. Technol. 183 (2007) 148–153.

[34] F. Liu, H. Yuan, J. Yin, J.T. Wang, Influence of stacking fault energy and temperature on microstructures and mechanical properties of fcc pure metals processed by equal-channel angular pressing, Mater. Sci. Eng. A. 662 (2016) 578–587.

[35] E.A. El-Danaf, M.S. Soliman, A.A. Almajd, EBSD investigation of the microstructure and microtexture evolution of 1050 aluminum cross deformed from ECAP to plane strain compression, J. Mater. Sci. 46 (2011) 3291–3308.

[36] W. Wei, K.X. Wei, G.J. Fan, A new constitutive equation for strain hardening and softening of fcc metals during severe plastic deformation, Acta Mater. 56 (2008) 4771–4779.

[37] S.M. Ashrafizadeh, A.R. Eivani, Correlative evolution of microstructure, particle dissolution, hardness and strength of ultrafine grained AA6063 alloy during annealing, Mater. Sci. Eng. A. 644 (2015) 284–296. doi:10.1016/j.msea.2015.06.074.

[38] P. Fornasini, The uncertainty in physical measurements: an introduction to data analysis in the physics laboratory, Springer Science & Business Media, 2008. https://books.google.com/books?hl=en&lr=&id=PBJgvPgf2NkC&oi=fnd&pg=PR7&dq=The+uncertainty+in+physical+measurements_+an+introduction+to+data+analysis+in+the+physics+laboratory&ots=Vca1FW7mv5&sig=91YiNskcX8V7QX6QVnj5seq8QGg (accessed September 27, 2016).

[39] E.A. El-Danaf, Texture evolution and fraction of favorably oriented fibers in commercially pure aluminum processed to 16 ECAP passes, Mater. Sci. Eng. A. 492 (2008) 141–152.

[40] A.P. Zhilyaev, D.L. Swisher, K. Oh-Ishi, T.G. Langdon, T.R. McNelley, Microtexture and microstructure evolution during processing of pure aluminum by repetitive ECAP, Mater. Sci. Eng. A. 429 (2006) 137–148.

[41] M. Torabi, A.R. Eivani, H.R. Jafarian, M.T. Salehi, Re-strengthening in AA6063 alloy during equal channel angular pressing, Journal of Ultrafine Grained and Nanostructured Materials, In press.